CXCL12 Mediates CCR7-independent Homing of Central Memory Cells, But Not Naive T Cells, in Peripheral Lymph Nodes

M. Lucila Scimone, Thomas W. Felbinger, Irina B. Mazo, Jens V. Stein, Ulrich H. von Andrian, and Wolfgang Weninger

The CBR Institute for Biomedical Research and the Department of Pathology, Harvard Medical School, Boston, MA 02115

Abstract

Central memory $CD8^+$ T cells (T_{CM}) confer superior protective immunity against infections compared with other T cell subsets. T_{CM} recirculate mainly through secondary lymphoid organs, including peripheral lymph nodes (PLNs). Here, we report that T_{CM}, unlike naive T cells, can home to PLNs in both a CCR7-dependent and -independent manner. Homing experiments in paucity of lymph node T cells (*plt/plt*) mice, which do not express CCR7 ligands in secondary lymphoid organs, revealed that T_{CM} migrate to PLNs at ~20% of wild-type (WT) levels, whereas homing of naive T cells was reduced by 95%. Accordingly, a large fraction of endogenous $CD8^+$ T cells in *plt/plt* PLNs displayed a T_{CM} phenotype. Intravital microscopy of *plt/plt* subiliac lymph nodes showed that T_{CM} rolled and firmly adhered (sticking) in high endothelial venules (HEVs), whereas naive T cells were incapable of sticking. Sticking of T_{CM} in *plt/plt* HEVs was pertussis toxin sensitive and was blocked by anti-CXCL12 (SDF-1α). Anti-CXCL12 also reduced homing of T_{CM} to PLNs in WT animals by 20%, indicating a nonredundant role for this chemokine in the presence of physiologic CCR7 agonists. Together, these data distinguish naive T cells from T_{CM}, whereby only the latter display greater migratory flexibility by virtue of their increased responsiveness to both CCR7 ligands and CXCL12 during homing to PLN.

Key words: lymphocytes • chemokines • migration • secondary lymphoid organs • recirculation

Introduction

Upon Ag encounter, naive T cells differentiate into effector cells poised to eradicate foreign or tumor Ags. Upon completing this task, most effector T cells die, leaving behind a small population of memory T cells that respond more rapidly to reencountered Ags (1–3). Based on the expression of certain adhesion molecules and chemokine receptors, two distinct subsets of memory T cells have been shown to arise during immune responses as follows: central memory T cells (T_{CM}) express L-selectin and CCR7 and localize to secondary lymphoid organs, whereas effector memory T cells (T_{EM}) are L-selectin$^-$CCR7$^-$ and found mainly in nonlymphoid tissues (4). When isolated from human blood, $CD8^+$ T_{EM} show greater cytotoxicity and produce more effector cytokines than T_{CM}. However, adoptive transfer of $CD8^+$ T_{CM} into naive recipients is more efficient than transfer of T_{EM} in conferring protective immunity. This may be due to the higher proliferative potential of T_{CM} as well as their greater capacity to persist in vivo (5). $CD8^+$ T_{EM} can differentiate into T_{CM} over several weeks; i.e., they reexpress L-selectin and CCR7 and acquire an enhanced capacity of homeostatic and Ag-driven proliferation (5). In addition, naive T cells can give rise to T_{CM} without first experiencing a full-fledged effector phase (6).

The localization of T_{CM} in LNs might further contribute to their key role in immune protection. Professional APCs,

M.L. Scimone and T.W. Felbinger contributed equally to this work.

Address correspondence to Ulrich H. von Andrian, The CBR Institute for Biomedical Research, 200 Longwood Ave., Boston, MA 02115. Phone: (617) 278-3130; Fax: (617) 278-3190; email: uva@cbr.med.harvard.edu

The present address of J.V. Stein is National Center for Biotechnology, CNB/CSIC, 28049 Madrid, Spain.

The present address of W. Weninger is The Wistar Institute, Philadelphia, PA 19104.

Abbreviations used in this paper: GFP, green fluorescent protein; GPCR, $G\alpha_i$-protein coupled receptor; HEV, high endothelial venule; IVM, intravital microscopy; MLN, mesenteric LN; PLN, peripheral LN; *plt*, paucity of lymph node T cells; PTX, pertussis toxin; T_{CM}, central memory T cells; T_{EM}, effector memory T cells; TRITC, tetramethylrhodamine-5-isothiocyanate.

in particular DCs, transport Ag from the periphery into the T cell zones of the LN (7). Thus, T_{CM} are strategically positioned to interact with DCs, which provide optimal stimulatory signals if T_{CM} detect a recall Ag on their surface.

We have recently described a method that allows for the generation of central memory–like $CD8^+$ T cells in vitro (6). Ag-primed $CD8^+$ T cells cultured in IL-15 for 5–7 d express high levels of CD44, L-selectin, and CCR7. Upon TCR stimulation, they produce IFN-γ, but are not acutely cytotoxic in vitro. After adoptive transfer, these cells survive for long periods of time, and mount rapid Ag-specific recall responses. We have shown that these cells migrate to all secondary lymphoid organs, including peripheral LNs (PLNs), mesenteric LNs (MLNs), Peyer's patches, and spleen (8). Similar to naive T cells, migration to PLNs occurred via high endothelial venules (HEVs) and depended on L-selectin (8).

To address the role of CCR7 in PLN homing, T_{CM} were injected into paucity of lymph node T cells (*plt/plt*) mice in which the lymphoid organ–expressed CCR7 ligands CCL19 (ELC) and CCL21-Ser (SLC) are deleted (9–12). The few T cells present in *plt/plt* PLNs are enriched for memory cells (10), shown here to be predominantly T_{CM}, indicating that this subset can home to LNs in the absence of CCR7 ligands. Indeed, although naive T cell homing was reduced to 5%, T_{CM} migration to *plt/plt* PLNs was reduced to only 20% of WT levels (8). This suggests involvement of one or more CCR7-independent pathways that enable at least some T_{CM} to home to PLNs.

In this paper, we show that T_{CM} rolled and adhered firmly in *plt/plt* PLN HEVs. T_{CM} sticking and migration to *plt/plt* PLNs were pertussis toxin (PTX) sensitive and CXCL12 dependent. Homing of T_{CM} to WT PLNs was also partially dependent on CXCL12. In contrast, CXCL12 had no detectable effect on naive T cell trafficking to PLNs. Thus, T_{CM} use at least two different chemokine pathways, CCR7–CCL19/21 and CXCR4–CXCL12, to enter PLNs under steady state conditions.

Materials and Methods

Mice

DDD/1-*plt/plt*, BALB/c-*plt/plt*, and DDD1-*mtv/mtv* control mice were provided by A. Matsuzawa (University of Tokyo, Tokyo, Japan). Transgenic T–green fluorescent protein (GFP) mice were generated in our laboratory (13). $CXCR3^{-/-}$ mice were provided by C. Gerard (Harvard University, Boston, MA). C57BL/6 and BALB/c mice were purchased from The Jackson Laboratory. Mice were housed and bred in a specific pathogen-free and viral antibody-free animal facility. Experiments were in accordance with National Institutes of Health guidelines and approved by the Committees on Animals of Harvard Medical School and The CBR Institute for Biomedical Research.

Reagents

Fluorochrome-labeled mAbs were obtained from BD Biosciences as follows: CD3ε, CD4, CD8α, CD44, CD25, L-selectin, CD122, CD69, and TCRβ. To detect CCR7 and P-selectin ligand expression, recombinant human CCL19-Ig and P-selectin–Ig chimeras were used (6). Antimurine CXCL12, recombinant murine CXCL12, CCL2, CCL5, CCL19, and recombinant human IL-15 were obtained from R&D Systems. PTX was obtained from Calbiochem.

In Vitro Differentiation of T_{CM}

T_{CM} were generated as described previously (6). In brief, splenocytes were incubated with 1 μg/ml anti-CD3ε and 2 d later with media containing 20 ng/ml IL-15 (for 5–8 d). Before each experiment, activation marker and homing molecule expression were assessed by flow cytometry (8).

ELISA and Immunofluorescence

PLNs were removed from WT and *plt/plt* mice, homogenized in lysis buffer (radioimmunoprecipitation assay buffer with 1 mM PMSF, 10 μg/ml aprotinin, and 10 μg/ml leupeptin), and centrifuged (14k *g* at 4°C for 10 min). The supernatant was assayed for CXCL12 immunoreactivity by ELISA (R&D Systems). Immunostaining of frozen sections was performed as described previously (14).

Homing Assays

Homing assays were performed as described previously (8). In brief, tetramethylrhodamine-5-isothiocyanate (TRITC)-labeled T_{CM} were mixed with LN cells from T-GFP mice and injected i.v. into recipients. After 1 or 24 h, 1 ml PBLs, spleen, PLNs, and MLNs were harvested, immunostained, and analyzed by flow cytometry. The homing index in organs was calculated as the ratio between the number of $CD8^+TRITC^+$ (T_{CM}) and $CD8^+GFP^+$ (naive) T cells divided by the ratio of $CD8^+TRITC^+$ and $CD8^+GFP^+$ cells in the input (8). In some experiments, T_{CM} were pretreated with 100 ng/ml PTX for 2 h before adoptive transfer. For blocking experiments, 100 μg/mouse anti-CXCL12 or control mAb were injected i.v. 15 min before adoptive transfer of T cells.

Intravital Microscopy and Image Analysis

Subiliac LN Preparation. Surgical preparation of LNs was performed as described previously (15). T_{CM} were labeled with calcein (Molecular Probes), and small boli of cells were injected intraarterially. T cell–endothelial cell interactions in subiliac LNs downstream from the injection site were recorded. For experiments testing the role of CXCL12, cell behavior was analyzed in the same vessels before and after mAb injection. To assess the role of $G\alpha_i$-protein coupled receptors (GPCRs), PTX-treated and untreated T_{CM} were compared.

Cremaster Muscle Preparation. Cremaster muscles of C57BL/6 mice were prepared as described previously (16). Calcein-labeled T_{CM} were injected, and several postcapillary and small collecting venules were recorded during a 15-min control period to determine baseline rolling and sticking. Subsequently, superfusion buffer was replaced with buffer containing 100 nM CXCL12, and T_{CM} behavior was recorded in the same vessels for an additional 15 min.

Offline frame-by-frame video analysis was performed as described previously (17). Rolling fraction was determined as the percentage of cells interacting with HEVs in the total number of cells passing through a vessel during the observation period. Sticking fraction was defined as the percentage of rolling cells that adhered in HEVs for ≥30 s.

Statistical Analysis. All data are presented as mean ± SEM. Homing indices were compared using the unpaired Student's *t*

test. Rolling and sticking fractions were compared using the paired Student's *t* test.

Results and Discussion

Preferential Recruitment of T_{CM} to plt/plt PLNs. T cells can enter LNs from the blood or via afferent lymphatic vessels draining tissues such as the skin (18). From the blood, naive T cells must adhere to HEVs, a process requiring L-selectin, CCR7, LFA-1, and their respective ligands (14, 18, 19). Similar to naive T cells, T_{CM} home to PLNs via HEVs in an L-selectin– and partially CCR7-dependent manner (8, 14, 19). Although naive T cells do not arrest in HEVs and home very poorly to *plt/plt* PLNs (14), T_{CM} are capable of entering these organs via HEVs, albeit considerably less efficiently than in WT mice (8). Competitive homing of naive T cells and T_{CM} in DDD/1-*plt/plt* mice revealed that the total number of homed naive T cells was reduced 19.2-fold compared with WT mice, whereas T_{CM} were only reduced by 4.9-fold (8). Recent observations suggest the defect in T cell migration to *plt/plt* LNs can vary with the genetic background (20). Thus, we repeated competitive homing assays in *plt/plt* mice on both BALB/c and DDD/1 backgrounds. In accordance with previous results (8), homing indices in BALB/c and DDD/1-*mtv/mtv* mice were 0.6 ± 0.1 and 0.4 ± 0.01, respectively; i.e., naive T cells accumulated approximately twofold more efficiently in WT PLNs than T_{CM} (Fig. 1, A and B). In contrast, homing indices were 1.4 ± 0.1 and 1.4 ± 0.2 in BALB/c-*plt/plt* and DDD/1-*plt/plt* PLN, respectively, indicating the CCR7 pathway may not be absolutely required for T_{CM} homing to PLNs. Both T_{CM} and naive T cells were equally affected in homing to MLNs in both DDD/1-*plt/plt* mice (by 89 and 88%, respectively) and BALB/c-*plt/plt* mice (by 92 and 94%, respectively). Thus, CCR7 is indispensable for T_{CM} trafficking to MLNs, whereas PLNs can recruit at least some T_{CM} in the absence of CCL19 and CCL21.

PLN in *plt/plt* mice are smaller than in WT animals, and contain a larger fraction of Ag-experienced lymphocytes (9, 10). However, the exact composition of memory T cells in these organs has not been determined. Because in vitro–generated T_{CM} retained, in part, the capacity to home to *plt/plt* PLNs, we examined the phenotype of resident $CD8^+$ memory T cells by staining BALB/c-*plt/plt* or BALB/c PLN single cell suspensions for CD122 (21). Expression of this memory marker correlated well with that of CD44 (Fig. 1 C). There was an approximately fivefold increase in the percentage of $CD8^+CD122^+$ T cells in *plt/plt* PLNs as compared with WT PLNs. Almost all of them expressed L-selectin and bound CCL19-Ig chimera, but little or no P-selectin–Ig, thus displaying a central memory phenotype (4). These observations strongly suggest that, in contrast to naive T cells, which depend almost entirely on CCR7 ligands, there may be a second homing pathway in PLNs that allows T_{CM} recruitment in the absence of CCL21 and CCL19.

T_{CM} Roll and Stick in plt/plt HEVs. There are two nonexclusive explanations for preferential T_{CM} traffic to *plt/plt* PLNs as follows: T_{CM} may have the unique ability to interact with HEVs by responding to an integrin-activating signal distinct from CCR7 ligands and/or they may enter via afferent lymphatic vessels. The latter mechanism was proposed by Mori et al., who observed delayed, but enhanced and prolonged T cell–mediated immune responses to contact sensitizers in *plt/plt* PLNs (22). Due to CCL21-leu expression in lymphatic vessels in *plt/plt* mice, both T

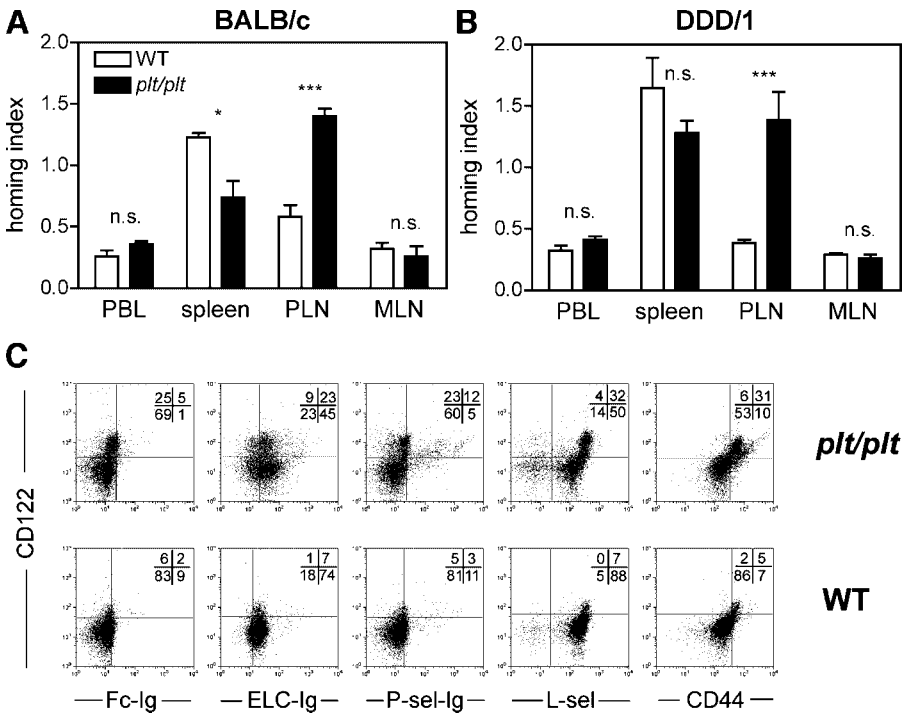

Figure 1. Accumulation of in vitro–cultured and endogenous T_{CM} in *plt/plt* PLNs. TRITC-labeled T_{CM} together with T-GFP LN cells were injected i.v. into BALB/c-*plt/plt* and BALB/c (A), and DDD/1-*plt/plt* and DDD/1-*mtv/mtv* mice (B). After 24 h, PBLs and secondary lymphoid organs were harvested, stained for CD8α, and analyzed by flow cytometry for the presence of $TRITC^+$ T_{CM} and naive GFP^+ T cells. Homing indices were calculated as described in Materials and Methods ($n = 6$ mice). n.s., not significant. *, $P < 0.05$; ***, $P < 0.001$. (C) Total PLN cells from *plt/plt* and WT mice were analyzed by flow cytometry. Representative dot plots from one experiment out of four are shown. Gates were set on $TCR\beta^+CD8\alpha^+$ cells. Numbers represent percentage of gated cells.

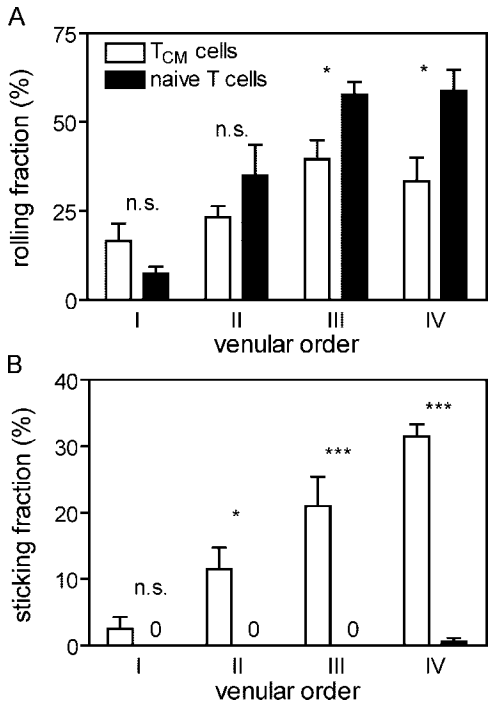

Figure 2. T_{CM} roll and stick in HEVs of *plt/plt* subiliac LNs. IVM analysis of calcein-labeled T_{CM} or naive GFP^+ T cells in DDD/1-*plt/plt* subiliac LNs. Interactions between fluorescent T cells and HEVs were visualized by epifluorescence IVM. Rolling (A) and sticking (B) fractions were determined for each venular order ($n = 6$ mice). n.s., not significant. *, $P < 0.05$; ***, $P < 0.001$.

cells and DCs can enter these vessels to migrate to PLNs (11, 22, 23). However, we show here that several T_{CM} accumulated in *plt/plt* PLNs as early as 1 h after i.v. injection. Given this brief interval, it seems unlikely that the homed cells could migrate to peripheral tissues and find their way into afferent lymphatics and from there into the cortex of draining LNs. Thus, our findings strongly suggest that T_{CM} can enter *plt/plt* PLN from the blood.

To test this hypothesis, we used intravital microscopy (IVM) to analyze T_{CM} behavior in the subiliac LN microcirculation of *plt/plt* mice. The venular tree of normal subiliac LNs consists of five successive venular branching orders, distinguishable by IVM (15). Order V represents postcapillary venules in the cortex and order I is the large collecting vessel at the LN hilus. In WT mice, naive T cells and T_{CM} roll and stick mainly in order III–V venules. These venules express the most peripheral node addressin, which mediates the rolling of L-selectin$^+$ T cells (8, 18, 19, 24). Firm adhesion requires activation of the integrin LFA-1 on rolling lymphocytes, which is usually induced by CCR7 ligands displayed in HEVs (14).

plt/plt PLNs are smaller than WT PLNs and their microarchitecture is disorganized, but the venular tree is readily discernible by IVM in DDD/1-*plt/plt* PLNs, even though order V venules are typically absent (14). By contrast, BALB/c-*plt/plt* PLNs are not amenable to IVM because the rarefied venular tree in this strain is obscured by overlying B cell follicles (14). Calcein-labeled T_{CM} were recorded in 43 HEVs (7 order I, 12 order II, 16 order III, and 8 order IV) in 6 DDD1-*plt/plt* mice (Fig. 2). Mean rolling fractions of T_{CM} were 17 ± 5% (order I), 23 ± 3% (order II), 40 ± 5% (order III), and 33 ± 7% (order IV). This is comparable to rolling fractions of T_{CM} in WT PLNs

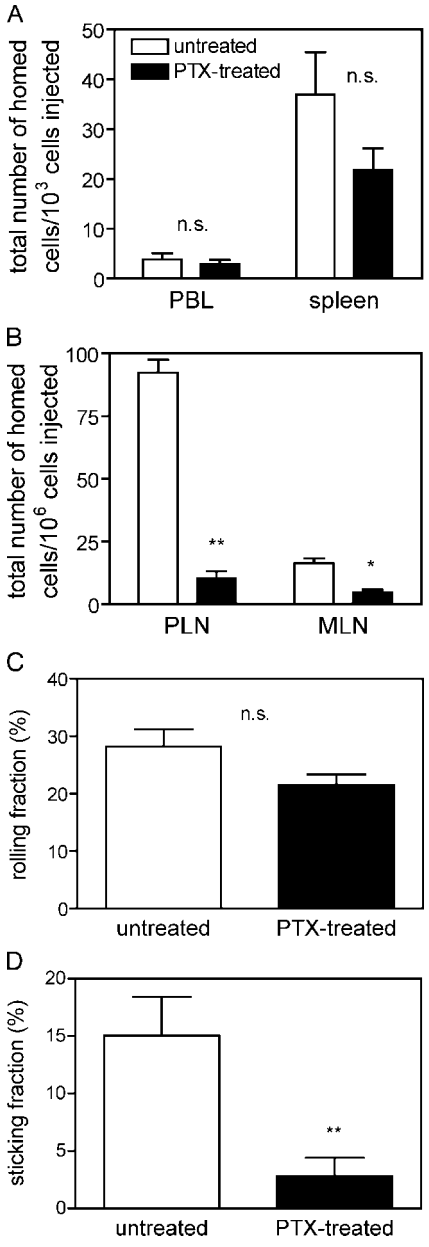

Figure 3. $G\alpha_i$-coupled signaling mediates CCR7-independent homing of T_{CM} to PLNs and is required for T_{CM} sticking in PLN HEVs of *plt/plt* mice. (A and B) TRITC-labeled control T_{CM} and CFSE-labeled PTX-treated T_{CM} were adoptively transferred into BALB/c-*plt/plt* recipients. After 24 h, PBLs, spleen, PLNs, and MLNs were harvested, and homed cells were analyzed by flow cytometry. Data are shown as the number of homed cells per 10^3 or 10^6 injected cells ($n = 3$ mice). (C and D) IVM analysis of rolling (C) and sticking fractions (D) of calcein-labeled control or PTX-treated T_{CM} in order III and IV HEVs in DDD/1-*plt/plt* PLNs ($n = 3$ mice). n.s., not significant. *, $P < 0.05$; **, $P < 0.01$.

(8). For comparison, naive GFP^+ T cells (14) were analyzed in 29 venules (2, order I; 8, order II; 8, order III; and 11, order IV) in seven mice. Their mean rolling fractions were 7 ± 2% (order I), 35 ± 9% (order II), 58 ± 4% (order III), and 59 ± 6% (order IV). Naive T cells rolled at similar frequencies in PLN HEVs of DDD/1-*plt/plt* and DDD/1-*mtv/mtv* mice, but completely failed to arrest in the former, indicating that CCR7 ligands are absolutely required (Fig. 2 and reference 14). However, T_{CM} were unmistakably capable of sticking in DDD/1-*plt/plt* PLN HEVs (Fig. 2 B, mean sticking fractions: order I, 2.5 ± 1.8%; order II, 11.5 ± 3.3%; order III, 21.0 ± 4.4%; and order IV, 31.5 ± 1.8%). We conclude that integrins are efficiently activated on rolling T_{CM} in *plt/plt* PLNs, indicating that an alternative chemoattractant pathway can be used by these cells. Moreover, HEVs are the likely port of PLN entry for T_{CM} in *plt/plt* mice.

Homing of T_{CM} to plt/plt PLN Is PTX Sensitive. Chemokine receptors are GPCRs whose function is efficiently blocked by PTX (25, 26). To determine whether CCR7-independent integrin activation signals on T_{CM} were perceived through such GPCRs, T_{CM} were preincubated with PTX before in vivo testing. PTX did not affect cell viability, but inhibited in vitro chemotaxis of T_{CM} toward CCL21 and CXCL12 by 80% (unpublished data). PTX treatment greatly reduced the ability of T_{CM} to home to BALB/c-*plt/plt* PLNs and MLNs, but had no effect on the number of T_{CM} in PBLs or spleen (Fig. 3, A and B). These results were further substantiated by IVM of DDD/1-*plt/plt* PLNs. There was no difference in the rolling fractions of PTX-treated and untreated T_{CM} (Fig. 3 C, mean: 22 ± 2% and 28 ± 3%, respectively; $P > 0.05$). This is not surprising because L-selectin–mediated rolling is insensitive to PTX (19). In contrast, the sticking fraction of control T_{CM} was fivefold higher than that of PTX-treated cells (Fig. 3 D, mean: 15.1 ± 3.4% and 2.8 ± 1.6%, respectively; $P < 0.01$). This indicates that one or more GPCRs, other than CCR7, mediates rapid integrin activation on rolling T_{CM} in PLN HEVs of *plt/plt* mice.

Homing of T_{CM} to DDD/1-plt/plt PLNs Is Partially Mediated by CXCL12. One chemoattractant candidate that could mediate T_{CM} homing to PLNs in the absence of CCR7 ligands is CXCL12. mRNA for CXCL12 is expressed by stromal cells in close vicinity to PLN HEVs, and CXCL12 protein was found in the lumen of some cortical HEVs (20). Moreover, CXCL12 and its receptor CXCR4 partly mediate homing of B cells to LN via HEV (20). In the case of T cell homing to *plt/plt* PLNs, the role of CXCR4–CXCL12 is more complex. Okada et al. found that $CXCR4^{-/-}$ T cells have no discernible defect in homing to WT PLNs, but $CXCR4^{-/-}$ splenic T cells were more severely compromised than WT T cells in their ability to migrate to *plt/plt* PLNs (20). Notably, the homing experiments with $CXCR4^{-/-}$ T cells were performed with total

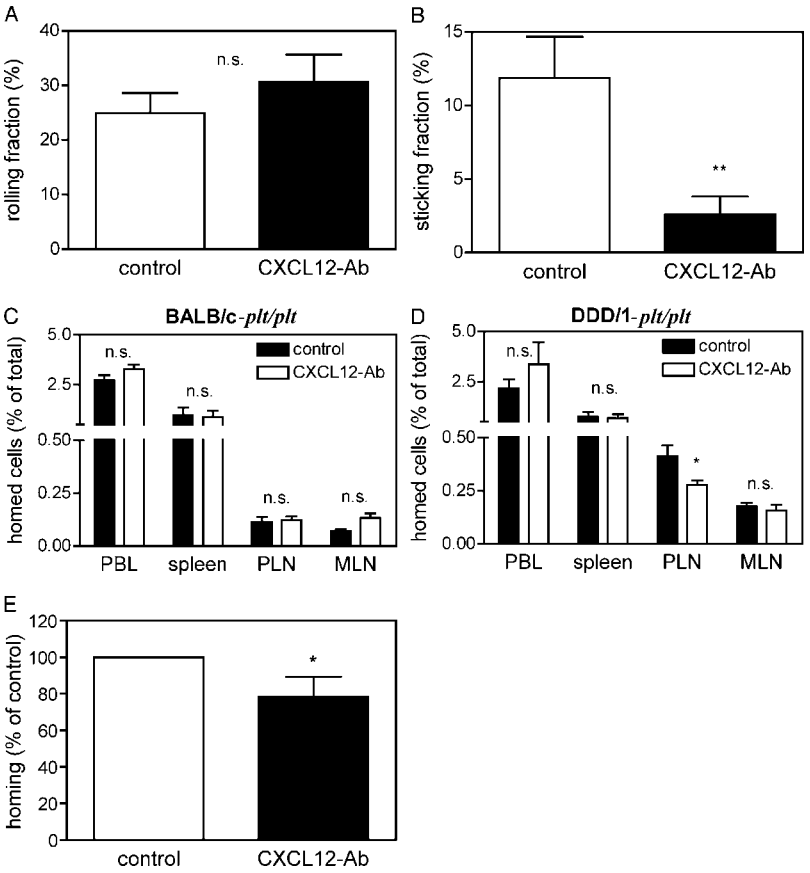

Figure 4. CXCL12 mediates CCR7-independent homing of T_{CM} to PLNs. (A and B) IVM analysis of rolling (A) and sticking fractions (B) of calcein-labeled T_{CM} in DDD/1-*plt/plt* PLN HEVs. Interactions of T_{CM} and HEVs in the same venules were recorded before and after injection of anti-CXCL12 ($n = 4$ mice). (C and D) TRITC-labeled T_{CM} were injected into BALB/c-*plt/plt* mice (C) or DDD/1-*plt/plt* mice (D) pretreated with control or anti-CXCL12 mAb. 1 h later, PBLs, spleen, PLNs, and MLNs were harvested and analyzed by flow cytometry. Data are expressed as percentage of homed cells in the total number of leukocytes ($n = 6$ mice). (E) TRITC-labeled T_{CM} were adoptively transferred into C57BL/6 mice injected previously with control or anti-CXCL12 mAb. 1 h later, PLNs were harvested and analyzed by flow cytometry. Data are expressed as percentage of homed cells relative to control mice ($n = 6$ mice). n.s., not significant. *, $P < 0.05$; **, $P < 0.01$.

splenocytes in which the T cell population typically contains ~30% memory cells. Conceivably, CXCL12-responsive T cells recovered from *plt/plt* PLNs by Okada et al. may have contained a disproportionate fraction of T_{CM}, rather than naive T cells, which predominate in WT PLNs.

Normal expression of CXCL12 in *plt/plt* PLNs makes this a good candidate for CCR7-independent T_{CM} migration to PLNs. Thus, we performed IVM of the subiliac LNs in DDD/1-*plt/plt* mice before and after anti-CXCL12 treatment. A total of 22 HEVs of orders III and IV in three DDD/1-*plt/plt* recipients were analyzed. Rolling fractions did not change after injection of anti-CXCL12 (Fig. 4 A, before: 25.0 ± 3.7%; after: 30.7 ± 5.0%; $P > 0.05$). In contrast, anti-CXCL12 markedly reduced the sticking fraction of T_{CM} from 11.9 ± 2.8% to 2.6 ± 1.2% (Fig. 4 B, $P < 0.01$). To determine whether CXCL12 mediates T_{CM} homing to *plt/plt* PLNs, anti-CXCL12 mAb was injected i.v. into DDD/1-*plt/plt* mice 15 min before injection of fluorescently tagged T_{CM}. Anti-CXCL12 had no effect on the accumulation of T_{CM} in PBLs, spleen, or MLNs after 1 h (Fig. 4, C and D). In contrast, the number of T_{CM} that homed to PLNs was ~30% lower than in control mice (Fig. 4 D, $P < 0.05$). We also performed competitive homing experiments using naive GFP^+ T cells and TRITC-labeled T_{CM} in DDD/1-*plt/plt* mice after anti-CXCL12 or control mAb injection ($n = 2$). Anti-CXCL12 did not alter the low number of naive T cells that homed to PLNs (unpublished data). However, consistent with the aforementioned data, the homing index decreased from 1.4 ± 0.1 to 1.0 ± 0.2, indicating that T_{CM}, but not naive T cells, home to PLNs in a partially CXCL12-dependent fashion. In contrast with DDD/1-*plt/plt* mice, anti-CXCL12 had no significant effect on T_{CM} homing to BALB/c-*plt/plt* PLNs (Fig. 4 C). As a possible explanation for this apparent discrepancy, we asked whether PLN HEVs in BALB/c-*plt/plt* mice present less CXCL12 on their luminal surface than their counterparts in DDD/1-*plt/plt*. However, ELISA of PLN lysates and immunostaining of frozen PLN sections from both strains did not reveal detectable differences in CXCL12 protein content and expression pattern, at least at the light microscopic level (unpublished data). Therefore, it is more likely that the lack of CXCL12 contribution to T_{CM} homing in BALB/c-*plt/plt* mice occurred because the venular tree in PLNs of this strain is very poorly developed compared with that in DDD/1-*plt/plt* (14). The available HEV surface area in the former may simply be too small to permit effective T_{CM} recruitment, despite CXCL12 expression. This explanation is consistent with the finding that the absolute number of T_{CM} that homed to BALB/c-*plt/plt* PLNs was three times lower than that recovered from DDD/1-*plt/plt* PLNs (85 ± 20 homed $T_{CM}/10^6$ injected cells versus 267 ± 116/10^6 injected cells, respectively; $P = 0.05$; Fig. 4, C and D, and not depicted).

Because our competitive homing experiments indicate that some T_{CM} home to BALB/c-*plt/plt* PLNs in a CCR7-independent fashion (Fig. 1 A), it is likely that one or more other chemoattractants may be expressed in PLN HEVs of BALB/c-*plt/plt* mice that mediate T_{CM} homing. The existence of additional GPCR-dependent recruitment signals appears likely, even in DDD/1 mice because PTX treatment blocked T_{CM} homing to PLNs in both *plt/plt* strains more completely than anti-CXCL12 (Fig. 3 B). Because in vitro–generated T_{CM} respond to CCL2 (monocyte chemoattractant protein–1) and CCL5 (regulated on activation, normal T cell expressed, and secreted [RANTES]; reference 8), we tested whether these chemokines contribute to T_{CM} homing to BALB/c-*plt/plt* PLNs. Furthermore, very low levels of CCL21-leu mRNA have been detected in *plt/plt* mice (27). Therefore, we desensitized T_{CM} with a 40-min incubation in 1 μM CCL2, CCL5, or CCL19 before adoptive transfer. The desensitized cells homed to BALB/c-*plt/plt* PLNs as efficiently as control cells (unpublished data), indicating that these chemokines do not play a role here. Other possible candidates include CXCR3 and its ligands as well as lipid chemoattractants, such as LTB4, which contribute to effector T cell homing to sites of inflammation (28). However, homing of $CXCR3^{-/-}$ T_{CM} was identical to that of WT T_{CM} (unpublished data), and T_{CM} do not chemotax toward LTB4 gradients (28). Thus, the nature of other chemoattractants involved in CCR7-independent T_{CM} homing to PLNs remains to be identified.

Together, these results strongly suggest that CXCL12–CXCR4 triggers integrin activation on rolling T_{CM}, but not on naive T cells, in PLN HEVs of DDD/1-*plt/plt* mice. This pathway accounts for a significant fraction of T_{CM} that home to PLNs. In addition, there is probably at least one other PTX-sensitive recruitment signal whose identity remains to be uncovered.

A Physiological Role for CXCL12 in T_{CM} Homing to PLNs. Given the severely disturbed architecture of secondary lymphoid organs in *plt/plt* mice (9, 10), we asked whether the observed contribution by CXCL12 to T_{CM} migration reflects a truly physiological event. Therefore, we examined the effect of CXCL12 inhibition on T_{CM} homing to WT PLNs. Indeed, homing was moderately by ~20%, but significantly, reduced (Fig. 4 E, $P < 0.05$). This reduction in homing occurred in both C57BL/6 and BALB/c mice, indicating that the role of CXCL12 in WT mice may not depend on genetic modifiers.

We conclude that the CCR7 pathway plays a dominant role in T_{CM} homing to PLNs, but CXCL12 also contributes to this process. Our finding that this nonredundant effect of CXCL12 is specific for T_{CM} is also supported by earlier conclusions that CXCR4 deficiency does not reduce the ability of naive T cells to home to PLNs that express normal CCR7 ligands (20).

CXCL12 Induces Firm Adherence of T_{CM}, But Not Naive T Cells, in Cremaster Muscle Venules. Why are naive T cells apparently incapable of using CXCL12 for homing to PLNs? Naive T cells respond to CXCL12 gradients in chemotaxis assays at least as efficiently as T_{CM} (unpublished data). Furthermore, CXCL12 induces LFA-1–mediated adhesion of human naive T cells to ICAM-1 in flow chamber assays (29). In contrast, murine naive T cells fail to ar-

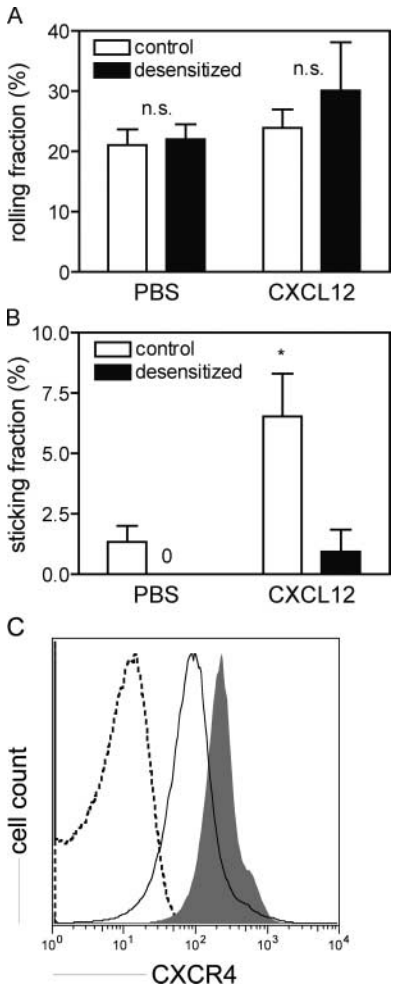

Figure 5. T_{CM} express higher levels of CXCR4 than naive T cells and stick in cremaster muscle venules upon topical exposure to CXCL12. Calcein-labeled untreated or CXCL12-desensitized T_{CM} were injected into a femoral artery of C57BL/6 mice, and rolling (A) and sticking (B) of fluorescent cells in cremaster muscle venules were recorded. Interactions between T_{CM} and the endothelium of the same muscle venules were recorded before and after superfusion of the preparation with 100 nM CXCL12 solution ($n = 3$ mice, 30 venules). *, $P < 0.05$. (C) Expression of CXCR4 on T_{CM} (shaded histogram) and $CD8^+$ naive T cells (solid line) was analyzed by flow cytometry. Isotype control staining is shown as a dotted line. Histograms are representative for results of $n = 2$. Gates were set on $TCR\beta^+CD8\alpha^+$ cells.

rest in cremaster muscle venules upon CXCL12 superfusion, but undergo immediate arrest in muscles superfused with CCL21 (16).

Because our homing data also indicate that CXCL12 fails to attract naive T cells to PLNs, but can recruit T_{CM}, we performed IVM to determine whether circulating T_{CM} can respond to CXCL12 in situ. To this end, we asked whether CXCL12 superfusion induces T_{CM} sticking in cremaster muscle venules (16). Fluorescently labeled T_{CM} were injected intraarterially and their interactions with cremaster muscle venules were recorded. Without CXCL12 superfusion, the mean rolling and sticking fractions were 18.3 ± 5.0% and 1.3 ± 0.9%, respectively ($n = 3$ mice/30 vessels). Upon subsequent superfusion with CXCL12, rolling fractions remained unchanged (Fig. 5 A, 23.9 ± 3.0%, $P > 0.05$). In contrast, the T_{CM} sticking fraction was significantly increased (Fig. 5 B, 6.9 ± 1.8%, $P < 0.05$ vs. control). To determine whether this was an effect of CXCL12 on the venular endothelium or on circulating T_{CM}, we desensitized T_{CM} to CXCL12 before injection. Desensitized T_{CM} rolled similarly to untreated cells, but were incapable of sticking (Fig. 5, A and B). Thus, T_{CM}, unlike naive T cells, are responsive to CXCL12 displayed on venular endothelium.

What could account for the distinct intravascular responsiveness of T_{CM} versus naive T cells to CXCL12? One possibility is that these two subsets express distinct densities of CXCR4. Indeed, flow cytometry revealed that T_{CM} expressed markedly higher levels of CXCR4 compared with naive $CD8^+$ T cells (Fig. 5 C; mean fluorescence intensity: T_{CM}, 278 and naive T cells, 126). This finding is also in accordance with a recent microarray analysis of T_{CM} and naive T cells, which showed higher mRNA expression of CXCR4 in the former subset (30).

What might be the functional relevance of CCR7-independent homing of T_{CM} to PLNs? Wherry et al. have recently shown that $CD8^+$ effector CTL can give rise to T_{EM}, which differentiate into L-selectin$^+$ T_{CM} over the course of several weeks (5). Effector CTL and T_{EM} do not express L-selectin and CCR7 (4, 6, 8). Although the kinetics of L-selectin and CCR7 induction on T_{EM} in the course of their transition into T_{CM} is unknown, it has been shown that some Ag-experienced T cells express L-selectin but not CCR7 (4). For this subset, expression of CXCR4 could provide an alternative pathway to gain CCR7-independent access to PLNs. Moreover, CXCL12 is constitutively expressed in many tissues, especially in the BM, and is upregulated during inflammation. In addition, human T_{CM} isolated ex vivo, and murine T_{CM} generated in vitro express several inflammatory chemokine receptors (4, 8). This broad expression pattern of chemokine receptors provides T_{CM} with maximum flexibility to survey not only secondary lymphoid organs but also multiple other sites in the body.

The authors thank L. Cavanagh and R. Bonasio for helpful discussions, A. Matsuzawa for *plt/plt* mice, C. Gerard for $CXCR3^{-/-}$ mice, B. Reinhardt and G. Cheng for technical support, and J. Moore for editorial assistance.

T.W. Felbinger was supported by a research stipend from the Deutsche Forshungsgemeinschaft. W. Weninger was supported by an Erwin-Schrödinger Auslandstipendium from the Austrian Science Foundation and by a Pilot and Feasibility grant from the Harvard Skin Disease Research Center. U.H. von Andrian was supported by National Institutes of Health grants HL48675, HL54936, and HL56949.

Submitted: 23 September 2003
Accepted: 4 March 2004

References

1. Sprent, J., and C.D. Surh. 2002. T cell memory. *Annu. Rev. Immunol.* 20:551–579.

2. Kaech, S.M., E.J. Wherry, and R. Ahmed. 2002. Effector and memory T-cell differentiation: implications for vaccine development. *Nat. Rev. Immunol.* 2:251–262.
3. Weninger, W., N. Manjunath, and U.H. von Andrian. 2002. Migration and differentiation of CD8+ T cells. *Immunol. Rev.* 186:221–233.
4. Sallusto, F., D. Lenig, R. Forster, M. Lipp, and A. Lanzavecchia. 1999. Two subsets of memory T lymphocytes with distinct homing potentials and effector functions. *Nature.* 401: 708–712.
5. Wherry, E.J., V. Teichgraber, T.C. Becker, D. Masopust, S.M. Kaech, R. Antia, U.H. von Andrian, and R. Ahmed. 2003. Lineage relationship and protective immunity of memory CD8 T cell subsets. *Nat. Immunol.* 4:225–234.
6. Manjunath, N., P. Shankar, J. Wan, W. Weninger, M.A. Crowley, K. Hieshima, T.A. Springer, X. Fan, H. Shen, J. Lieberman, and U.H. von Andrian. 2001. Effector differentiation is not prerequisite for generation of memory cytotoxic T lymphocytes. *J. Clin. Invest.* 108:871–878.
7. Banchereau, J., and R.M. Steinman. 1998. Dendritic cells and the control of immunity. *Nature.* 392:245–252.
8. Weninger, W., M.A. Crowley, N. Manjunath, and U.H. von Andrian. 2001. Migratory properties of naive, effector, and memory $CD8^+$ T cells. *J. Exp. Med.* 194:953–966.
9. Nakano, H., T. Tamura, T. Yoshimoto, H. Yagita, M. Miyasaka, E.C. Butcher, H. Nariuchi, T. Kakiuchi, and A. Matsuzawa. 1997. Genetic defect in T lymphocyte-specific homing into peripheral lymph nodes. *Eur. J. Immunol.* 27:215–221.
10. Nakano, H., S. Mori, H. Yonekawa, H. Nariuchi, A. Matsuzawa, and T. Kakiuchi. 1998. A novel mutant gene involved in T-lymphocyte-specific homing into peripheral lymphoid organs on mouse chromosome 4. *Blood.* 91:2886–2895.
11. Luther, S.A., H.L. Tang, P.L. Hyman, A.G. Farr, and J.G. Cyster. 2000. Coexpression of the chemokines ELC and SLC by T zone stromal cells and deletion of the ELC gene in the plt/plt mouse. *Proc. Natl. Acad. Sci. USA.* 97:12694–12699.
12. Vassileva, G., H. Soto, A. Zlotnik, H. Nakano, T. Kakiuchi, J.A. Hedrick, and S.A. Lira. 1999. The reduced expression of 6Ckine in the plt mouse results from the deletion of one of two 6Ckine genes. *J. Exp. Med.* 190:1183–1188.
13. Manjunath, N., P. Shankar, B. Stockton, P.D. Dubey, J. Lieberman, and U.H. von Andrian. 1999. A transgenic mouse model to analyze CD8+ effector T cell differentiation in vivo. *Proc. Natl. Acad. Sci. USA.* 96:13932–13937.
14. Stein, J.V., A. Rot, Y. Luo, M. Narasimhaswamy, H. Nakano, M.D. Gunn, A. Matsuzawa, E.J. Quackenbush, M.E. Dorf, and U.H. von Andrian. 2000. The CC chemokine thymus-derived chemotactic agent 4 (TCA-4, secondary lymphoid tissue chemokine, 6Ckine, exodus-2) triggers lymphocyte function-associated antigen 1–mediated arrest of rolling T lymphocytes in peripheral lymph node high endothelial venules. *J. Exp. Med.* 191:61–76.
15. von Andrian, U.H. 1996. Intravital microscopy of the peripheral lymph node microcirculation in mice. *Microcirc.* 3:287–300.
16. Weninger, W., H.S. Carlsen, M. Goodarzi, F. Moazed, M.A. Crowley, E.S. Baekkevold, L.L. Cavanagh, and U.H. von Andrian. 2003. Naive T cell recruitment to non-lymphoid tissues: a role for endothelium-expressed CCL21 in autoimmune disease and lymphoid neogenesis. *J. Immunol.* 170: 4638–4648.
17. von Andrian, U.H., and C. M'Rini. 1998. In situ analysis of lymphocyte migration to lymph nodes. *Cell Adhes. Commun.* 6:85–96.
18. von Andrian, U.H., and T.R. Mempel. 2003. Homing and cellular traffic in lymph nodes. *Nat. Rev. Immunol.* 3:867–878.
19. Warnock, R.A., S. Askari, E.C. Butcher, and U.H. von Andrian. 1998. Molecular mechanisms of lymphocyte homing to peripheral lymph nodes. *J. Exp. Med.* 187:205–216.
20. Okada, T., V.N. Ngo, E.H. Ekland, R. Forster, M. Lipp, D.R. Littman, and J.G. Cyster. 2002. Chemokine requirements for B cell entry to lymph nodes and Peyer's patches. *J. Exp. Med.* 196:65–75.
21. Zhang, X., S. Sun, I. Hwang, D.F. Tough, and J. Sprent. 1998. Potent and selective stimulation of memory-phenotype CD8+ T cells in vivo by IL-15. *Immunity.* 8:591–599.
22. Mori, S., H. Nakano, K. Aritomi, C.R. Wang, M.D. Gunn, and T. Kakiuchi. 2001. Mice lacking expression of the chemokines CCL21-ser and CCL19 (plt mice) demonstrate delayed but enhanced T cell immune responses. *J. Exp. Med.* 193:207–218.
23. Nakano, H., and M.D. Gunn. 2001. Gene duplications at the chemokine locus on mouse chromosome 4: multiple strain-specific haplotypes and the deletion of secondary lymphoid-organ chemokine and EBI-1 ligand chemokine genes in the plt mutation. *J. Immunol.* 166:361–369.
24. Stockton, B.M., G. Cheng, N. Manjunath, B. Ardman, and U.H. von Andrian. 1998. Negative regulation of T cell homing by CD43. *Immunity.* 8:373–381.
25. Springer, T.A. 1994. Traffic signals for lymphocyte recirculation and leukocyte emigration: The multi-step paradigm. *Cell.* 76:301–314.
26. Spangrude, G.J., B.A. Braaten, and R.A. Daynes. 1984. Molecular mechanisms of lymphocyte extravasation. I. Studies of two selective inhibitors of lymphocyte recirculation. *J. Immunol.* 132:354–362.
27. Gunn, M.D., S. Kyuwa, C. Tam, T. Kakiuchi, A. Matsuzawa, L.T. Williams, and H. Nakano. 1999. Mice lacking expression of secondary lymphoid organ chemokine have defects in lymphocyte homing and dendritic cell localization. *J. Exp. Med.* 189:451–460.
28. Goodarzi, K., M. Goodarzi, A.M. Tager, A.D. Luster, and U.H. Von Andrian. 2003. Leukotriene B4 and BLT1 control cytotoxic effector T cell recruitment to inflamed tissues. *Nat. Immunol.* 4:965–973.
29. Campbell, J.J., J. Hedrick, A. Zlotnik, M.A. Siani, D.A. Thompson, and E.C. Butcher. 1998. Chemokines and the arrest of lymphocytes rolling under flow conditions. *Science.* 279:381–384.
30. Kaech, S.M., S. Hemby, E. Kersh, and R. Ahmed. 2002. Molecular and functional profiling of memory CD8 T cell differentiation. *Cell.* 111:837–851.